



LAWRENCE  
LIVERMORE  
NATIONAL  
LABORATORY

# In-situ monitoring of flow-permeable surface area of high explosive powder using small sample masses

R. H. Gee, T. Y. Han, F. Zaka, A. Maiti

November 5, 2014

Propellants, Explosives, Pyrotechnics

## **Disclaimer**

---

This document was prepared as an account of work sponsored by an agency of the United States government. Neither the United States government nor Lawrence Livermore National Security, LLC, nor any of their employees makes any warranty, expressed or implied, or assumes any legal liability or responsibility for the accuracy, completeness, or usefulness of any information, apparatus, product, or process disclosed, or represents that its use would not infringe privately owned rights. Reference herein to any specific commercial product, process, or service by trade name, trademark, manufacturer, or otherwise does not necessarily constitute or imply its endorsement, recommendation, or favoring by the United States government or Lawrence Livermore National Security, LLC. The views and opinions of authors expressed herein do not necessarily state or reflect those of the United States government or Lawrence Livermore National Security, LLC, and shall not be used for advertising or product endorsement purposes.

# In-situ monitoring of flow-permeable surface area of high explosive powder using small sample masses

Amitesh Maiti, Yong Han, Fowzia Zaka, and Richard H. Gee\*

Lawrence Livermore National Laboratory, Livermore CA 94550

Email: gee10@llnl.gov

## **Abstract:**

To ensure good performance of high explosive devices over long periods of time, initiating powders need to maintain their specific surface area within allowed margins during the entire duration of deployment. A common diagnostic used in this context is the Fisher sub-sieve surface area (FSSA). Commercial permeametry instruments measuring the FSSA requires the utilization of a sample mass equal to the crystal density of the sample material, an amount that is often one or two orders of magnitude larger than the typical masses found in standard detonator applications. Here we develop a customization of the standard device that can utilize just tens of milligram samples, and with simple calibration yield FSSA values at accuracy levels comparable to the standard apparatus. This necessitated a newly designed sample holder, made from a material of low coefficient of thermal expansion, which is conveniently transferred between an aging chamber and a re-designed permeametry tube. This improves the fidelity of accelerated aging studies by allowing measurement on the same physical sample at various time-instants during the aging process, and by obviating the need for a potentially FSSA-altering powder re-compaction step. We used the customized apparatus to monitor the FSSA evolution of a number of undoped and homolog-doped PETN powder samples that were subjected to artificial aging for several months at elevated temperatures. These results, in conjunction with an Arrhenius-based aging model were used to assess powder-coarsening-rates under long-term storage.

**Keywords:** Specific surface area, Flow permeametry, Powder coarsening

## 1. Introduction and Motivation

Ignition characteristics of many high explosive devices following long-term storage hinges critically on the maintenance of the specific surface area (i.e. surface area per unit mass) of initiating powders like pentaerythritol tetranitrate (PETN) and octogen (more commonly known as Her Majesty's Explosive or HMX) [1-6]. Experimental evidence indicates that over time such powders tend to coarsen, thereby leading to a reduction in the specific surface area [7]. Over a period of decades the specific surface area may fall to low enough levels so as to adversely affect device functioning. The most common quantitative way to characterize specific surface area in connection with ignition properties is through flow permeametry, where the rate of flow of a fluid (e.g. air) through a sample powder bed is converted to an average particle size [8], which in turn can be expressed as a specific surface area. The most common commercial apparatus performing such characterization is the Fisher sub-sieve sizer, and below we refer the specific surface area determined by this apparatus as the Fisher sub-sieve surface area (FSSA).

For reasons made clear in section 2, the standard commercial apparatus employs powder sample of mass equal to that of  $1 \text{ cm}^3$  of the crystalline material, which for the explosives PETN and HMX (assuming  $\beta$ -HMX) amount to  $\sim 1.78 \text{ g}$  and  $\sim 1.91 \text{ g}$ , respectively. Note that it is often the case that the amount of explosive powder available to perform a FSSA measurement is much less than is required, of the order of only 100 mg or so. Additionally, in accelerated aging studies where one monitors the evolution of FSSA as a function of time and temperature, the standard permeametry apparatus has two procedural drawbacks: (1) FSSA measurement at different time-instants during aging involves different physical aliquots extracted from a larger sample that is being subjected to accelerated aging; and (2) during the transfer of the aliquot from the aging chamber to the Fisher tube the powder in the aliquot is re-compacted into the sample holder of the tube, a procedure that could potentially alter the FSSA value.

The purpose of this work is to demonstrate a simple modification to the apparatus that can be used with much less explosive powder, which at the same time overcomes both drawbacks of the standard apparatus mentioned above. The re-designed permeametry tube and sample holder (hereafter to be referred to as modified-Fisher) can work with only  $\sim 100 \text{ mg}$  PETN powder samples and yet yield consistent FSSA

values at accuracy levels comparable to that of the unmodified commercial apparatus. The sample holder itself can be conveniently transferred between the aging chamber and the re-designed permeametry tube. This ensures that the same physical sample is used to monitor FSSA evolution with time, and avoids the need for powder re-compaction during transfer from the aging chamber to the permeametry tube. The rest of the paper is organized as follows: Section 2 lays out the permeametry theory behind the working of the standard Fisher apparatus; section 3 provides some of the design details of the re-designed permeametry tube and sample holder; section 4 discusses a simple linear calibration that is necessary to bring the small-mass FSSA (measured by modified-Fisher) in correspondence to the FSSA measured in its standard configuration; and section 5 displays results on FSSA evolution of both undoped and homolog-doped PETN samples as measured by modified-Fisher, from which predictions on long-term aging are made using an Arrhenius-based model.

## 2. Theory behind standard Fisher sub-sieve sizer

The FSSA is based on the theory of fluid flow through a bed of the porous sample powder. Assuming flow in the viscous regime, the average speed of flow normal to the bed ( $\langle u \rangle$ ) is related to the pressure difference ( $\Delta p$ ) across the powder bed thickness ( $L$ ), dynamic viscosity of the fluid ( $\eta$ ), powder surface area and density, and the average tortuosity ( $\tau$ ) of the flow path. Starting from the standard Poiseuille's equation for laminar flow Carman and Kozeny derived such a relation [9-11]. Expressing the powder density in terms of its porosity or void fraction ( $\varepsilon$ ) and the specific surface area in terms of an average spherical particle diameter ( $d_s$ ), the Carman-Kozeny equation in its standard form is written as:

$$\langle u \rangle = \frac{\Delta p}{L} \frac{d_s^2}{72\tau\eta} \frac{\varepsilon^3}{(1-\varepsilon)^2} \quad (1)$$

It should be noted that although eqn. (1) was originally developed for the flow of incompressible liquids, they also apply to the flow of compressible fluids like air as long as the pressure drop across the sample is much less than the overall background pressure, which is true under standard operations of the Fisher instrument (see below). Otherwise one needs a pressure-correction term [8].

Solving eq. (1) one obtains the following expression for the average spherical particle size  $d_s$ :

$$d_s = C_1 \sqrt{C_{sample} \frac{L (1-\varepsilon)^2}{A \varepsilon^3}}, \quad (2)$$

where intrinsic (geometry-independent) factors like tortuosity, fluid viscosity, etc. have been lumped into the pre-factor  $C_1$ ,  $A$  is the cross-section area of the sample, and  $C_{sample} = \frac{\langle u \rangle A}{\Delta p}$  is a measure of the flow *conductance* through the sample.

In the Fisher apparatus there is an additional reference porous plug of known flow conductance  $C_{reference}$  placed in series with the sample bed. The total pressure drop ( $P$ ) across the two beds (sample + reference plug) is then a sum of two drops:  $(P - F)$  across the sample +  $F$  across the reference plug. Under standard operation air is the flowing fluid, and the total pressure drop ( $P$ ) is maintained at 50 mm of water, which is much smaller than the overall background pressure of 1 atm. Thus, the volume changes of air while flowing through the two plugs is small and typically ignored. Thus, conservation of mass implies that the rate of volume flow through the two plugs is the same, i.e.,  $C_{sample}(P - F) = C_{reference}F$ . Eliminating  $C_{sample}$  from eq. (2) and collecting  $C_{reference}$  and other geometry-independent constants into a constant  $C$ , one then obtains:

$$d_s = C \sqrt{\frac{L (1-\varepsilon)^2}{A \varepsilon^3} \frac{F}{(P-F)}}, \quad (3)$$

which is a form of the Gooden-Smith equation [12] on which the operation of the commercial Fisher instrument is based.

The standard Fisher apparatus uses a powder sample mass equivalent to that of 1 cm<sup>3</sup> of the crystalline material (for PETN this corresponds to a sample mass of 1.78 g), from which  $L$  can be determined for a given  $A$  and  $\varepsilon$ . Then from known instrument constant ( $C$ ), known tube cross-section ( $A$ ), known  $P$  (i.e., 50 mm of water), and measured  $F$  via the height of a water meniscus, the average spherical particle diameter  $d_s$  can be determined for a given porosity level  $\varepsilon$ . The Fisher instrument provides a chart with iso- $d_s$  curves,

from which the user can directly read the value of  $d_s$  from the observed height of a water meniscus. At the same time, eq. (3) shows that for a given porosity level  $\varepsilon$ , the functional dependence of  $d_s$  on  $F$  is independent of the tube dimensions and sample mass as long as a fixed ratio of  $L/A$  is maintained. In other words, even for much smaller sample masses (as compared to that used in the standard apparatus) loaded in a smaller tube (so as to maintain a target value of  $\varepsilon$ ), the same iso- $d_s$  curves provided with the standard instrument can be used to read  $d_s$  directly, as long as the same  $L/A$  ratio is maintained. Finally, from the average spherical diameter  $d_s$ , the Fisher sub-sieve surface area (FSSA) is simply computed as:

$$FSSA = \frac{6}{\rho_s d_s} \quad , \quad (4)$$

where  $\rho_s$  is the crystal density of the material (e.g. 1.78 g/cm<sup>3</sup> for PETN).

### 3. Modified apparatus design

Fig. 1 provides a schematic description of the re-designed permeametry tube and sample holder. In order to utilize available sample masses of 111 mg for FSSA measurements we machined a cylindrical sample holder of diameter 6.35 mm and length  $L = 3.71$  mm. The dimensions were chosen so as to maintain the same  $L/A$  ratio as the original Fisher tube (see discussion at the end of the previous section), and at the same time to ensure a porosity level of  $\varepsilon = 0.468$ , consistent with what has been used historically in prior PETN studies [14]. However, as mentioned at the outset, the purpose of designing a small sample holder was not just to be able to work with small sample masses, but also to be able to carry out effectively *in-situ* monitoring of FSSA evolution of powder samples as a function of time and temperature while avoiding any mechanical disturbance that might affect the powder surface area. This is accomplished by first pressing the PETN powder into the sample holder and then placing into the re-designed permeametry tube to measure the powders FSSA. Once the FSSA of the powder sample has been measured, the sample is placed into the Invar aging assembly for aging. The Invar aging assembly was designed so as to confine the sample in a configuration representative of its application in a detonator, and thus maintain an equilibrium vapor pressure of PETN during aging. The sample holder and aging assembly were made from

Invar due to its low coefficient of thermal expansion. This is critical in minimizing the possibility of the formation of leak paths that may form at the interface between the pressed powder sample (PETN powder as used here) and the Invar sample holder. At various time-points during aging the sample holder is briefly transferred from the aging assembly to the permeametry tube for FSSA measurement with modified-Fisher, and then transferred back to the aging assembly for continued aging. Various features of the re-designed permeametry tube shown in Fig. 1 are worth mentioning: (1) the filter paper discs between the loaded sample holder and the permeametry tube are inserted as a precautionary step to help protect the powder sample from being mechanically disturbed; (2) the addition of the o-ring between the sample holder and the air inlet side of the permeametry tube is to ensure an air-tight seal between the incoming air flow and the powder sample, and (3) springs are added to the sample holder housing to facilitate easy insertion and removal of the holder. Few studies exist on the in-situ surface area analysis for detonators, although one from AWE, UK deserves special mention [13].

#### 4. Calibration of the modified apparatus

As mentioned in the previous sections, the average spherical particle diameter  $d_s$  read from the standard iso- $d_s$  curves using a much smaller Fisher tube (i.e. employing a much smaller amount of sample mass) should, in principle, be the same as that obtained using the recommended  $\rho_s$  grams of sample mass as long as the same  $L/A$  ratio is maintained (at a fixed target porosity level). However, this assumes that the constant  $C$  in eq. (3), which consists of various flow parameters in the model (e.g., flow conductance  $C_{reference}$ , air viscosity, flow tortuosity, and various other constants) does not depend on the volume rate of air flow. In reality, one expects some dependence on the volume flow. Thus it became necessary to calibrate the FSSA results from the modified-Fisher relative to those measured by the standard instrument.

Fig. 2 displays the  $d_s$  results for eight different PETN powders using the modified-Fisher (x-axis) using 111 mg of powder and the standard Fisher (y-axis) using 1.78 g of powder. Although the precision limits in  $d_s$  leads to some scatter in the data, there is clearly a very strong linear correlation (> 98%) between the two sets of measurements. Thus, for standardization, all measurements using the modified-Fisher (reported below) were recalibrated using the slope of Fig. 2.

## 5. Aging results for various powders – effects of homolog-doping on powder coarsening

In a prior publication [15] we used historical accelerated PETN aging data to develop an aging model for pure PETN. The model utilized exponential functions and an Arrhenius behavior to fit the accelerated aging data. For pure PETN the model predicted a decrease in specific surface area between 2-6% in 50 years under ambient conditions. However, the functional form used was not physically motivated. In particular, two different functions were used to fit the initial rapid coarsening and the later gradual coarsening, and the activation barriers did not represent any physical process that one could identify as the dominant coarsening mechanism. In this work we have decided to use a single function with a single activation barrier representing the dominant physical mechanism. After analyzing available accelerated aging data of a number of PETN powders, the following functional form appeared suitable:

$$\frac{FSSA(t)}{FSSA(0)} = \left(1 + \frac{t}{\tau}\right)^{-\alpha}, \quad (5)$$

where  $\tau$  is a measure of the time-scale over which significant coarsening occurs,  $\alpha$  is a (positive) constant, and  $FSSA(0)$  is the Fisher sub-sieve surface area at the beginning of coarsening. In the above model  $\alpha$  can depend strongly on the nature of the powder (e.g., whether homolog-doped) but otherwise assumed temperature-independent, while the time-scale  $\tau$  is assumed to follow an Arrhenius behavior, i.e.,

$$\tau = \tau_{\infty} \exp(\Delta E / k_B T), \quad (6)$$

where  $\Delta E$  is the activation barrier,  $k_B$  the Boltzmann constant,  $T$  the temperature in the Kelvin scale, and  $\tau_{\infty}$  a constant signifying the value of coarsening timescale  $\tau$  at very high temperatures. Given that the experimental literature on the coarsening of PETN powder has primarily focused on sublimation-dominated processes [7, 16, 17], we assumed  $\Delta E = 35.1$  kcal/mol, an accepted value for PETN's sublimation energy.

To check the applicability of the above model in describing powder coarsening behavior typically observed with PETN, eqs. (5) and (6) were first used to fit historical coarsening data (see Ref. [15]), as

shown in Fig. 3. With parameters  $\alpha$  and  $\tau_\infty$  optimized for the smallest RMS deviation from this experimental data, the new aging model was then used to predict the PETN powder coarsening over a period of decades at room temperature ( $T = 25$  °C). As Fig. 4 indicates, the predicted drop in FSSA after 50 years is  $\sim 4\%$ , very comparable to the 2-6% drop predicted by our earlier model.

Next, we used the present model to analyze accelerated aging results for both doped and undoped PETN powders. Below we analyze four different powder systems, which we call powder A, B, C and D, respectively. The first two powders (A and B) were pure (i.e., undoped) PETN, while powders C and D were doped with approximately 1 wt% of PETN's trimer homolog, TriPEON (tripentaerythritol octanitrate) (see Fig. 5). There were six samples corresponding to each powder system. We observed systematic differences between the sample-averaged FSSA values of the as-obtained powders (i.e. before accelerated aging was started), probably due to differences in their initial preparation and thermal history. Thus the sample-averaged initial FSSA values of the four powder systems A, B, C, and D were about 0.73, 0.63, 0.65, and 0.59  $\text{m}^2/\text{g}$ , respectively. Given that each sample consisted of a small amount of powder, 111 mg each, all these FSSA values (and the FSSA of aged powders reported below) were obtained by measurements using the modified-Fisher followed by recalibration with the slope of Fig. 2, as discussed in the previous section.

In the accelerated aging experiments all 24 samples were subjected to a constant temperature of 70 °C for 100 days. For each sample the FSSA was recorded at several specified times during the aging process. Figs. 6 and 7 display the resulting evolution of FSSA for the undoped (A and B) and TriPEON-doped (C and D) powders, respectively, with each sample's FSSA normalized by  $\text{FSSA}(0)$ , i.e., the FSSA value at the beginning of accelerated aging. Results for all samples have been included in our analysis except for sample 1 of powder C and sample 6 of powder D, which gave inconsistent results (e.g., FSSA increased with aging, likely due to a bad initial FSSA measurement rather than an actual increase in FSSA). Upon comparing Figs. 6 and 7 it is evident that powders C and D display much less coarsening as compared to powders A and B. In other words, the presence of TriPEON in powders C and D significantly slows down PETN coarsening kinetics.

Given that our earlier experiments using thermo-gravimetric analysis (TGA) [18] suggests little change in activation barrier due to doping with homologs like TriPEON and DiPEHN (dipentaerythritol hexanitrate), we used  $\Delta E = 35.1$  kcal/mol for all powders studied in this work. Thus for long-term predictions, only parameters  $\alpha$  and  $\tau_\infty$  were needed to be optimized for each powder corresponding to the smallest RMS deviation from the accelerated aging data. The resulting model values are indicated by the solid lines in Figs. 6 and 7. These optimized parameters were then used with eqs. (5) and (6) to predict the coarsening behavior (in terms of FSSA evolution) for powders A, B, C, and D at 25 °C over a period of decades. Fig. 8 displays the long-term predictions for all four powder systems, plus the historical powder (Ref. [15]) from Fig. 4. The predicted drop in FSSA in 50 years under ambient conditions (25 C) is: the historical powder (4%), powder A (8.7%), powder B (3.4%), powder C (1%), and powder D (0.7 %). The increased predicted coarsening in powder A (as compared to powder B) could be due to the fact that these powders had a higher initial surface area ( $FSSA(0) = 7300$  cm<sup>2</sup>/g), which indicates insufficient annealing during its preparation and a consequent higher propensity for coarsening. The same argument could probably be used to explain the differences in the predicted coarsening between powders C and D, although their differences are much smaller.

## 5. Summary

To summarize, we employed the original Gooden-Smith equation to modify the commercial Fisher apparatus to be used with much smaller amounts of powder than the mass-equivalent of 1 cm<sup>3</sup> of powder at crystal density that the standard apparatus is calibrated for. More specifically, we show that the same iso- $d_s$  curves provided with the standard instrument can be used to read off an average spherical particle diameter (and from that FSSA determined via eq. (4)) as long as the same  $L/A$  ratio as in the standard settings is maintained. This extension allows FSSA measurements of powders that are of limited availability. For PETN, the resulting FSSA values using 111 mg of powder samples showed a strong linear correlation with the FSSA values obtained using the standard recommended 1.78 g of powder. This enabled obtaining FSSA values using the smaller amounts of powder with a simple recalibration. Using the modified instrument we studied the evolution of FSSA of multiple samples of four different powders: two undoped, and two doped

with 1 wt% TriPEON, all subjected to an elevated temperature of 70 °C for 100 days. Using an Arrhenius-based aging model we used this data to predict the long-term coarsening of these powders for a period of several decades under ambient conditions. In 50 years, appropriately prepared undoped PETN (powder system B) is predicted to undergo FSSA reduction (i.e. coarsening) by ~ 3.4%, which is comparable to what is predicted for historical data presented in Ref. [15] (4%), while TriPEON-doped powders (powder systems C and D) are predicted to coarsen much less, by 1% or less. On the other hand, for powder prepared with insufficient annealing (presumably the case with powder system A) the coarsening could be faster, by as much 8.7% in 50 years.

***Acknowledgement:*** This work was performed under the auspices of the U.S. Department of Energy by Lawrence Livermore National Laboratory under Contract DE-AC52-07NA27344.

## References:

1. R. Meyer, J. Kçhler, A. Homburg (Eds.), Explosives, Weinheim, Germany Wiley-VCH, 6th Edition, 2007.
2. R. H. Dinegar, R. H. Rochster, M. S. Millican, The effect of specific surface on the explosion times of shock initiated PETN, *Am. Chem. Soc. Div. Fuel Chem.* **1963**, 7, 17.
3. J. A. Waschl, An investigation of PETN sensitivity to small scale flyer plate impact, *J. Energetic Mater.* **1998**, 16, 279.
4. J. W. Rogers and A. A. Duncan, Effects of Particle Characteristics on Performance of RR5K PETN, Albuquerque, NM: Sandia National Laboratories/New Mexico, **1981**. SAND81-2199. Available from NTIS, Springfield, VA.
5. R. H. Dinegar, The Effect of Heat on PETN, Proceedings of the 3rd International Conference of Groupe de Travail de Pyrotechnie, Juan-Lespin, France, Assoc. Francaise de Pyrotechnie, Paris. **1989**.
6. M. F. Foltz, Aging of Pentaerythritol Tetranitrate (PETN), LLNL-TR-415057, **2009**.
7. H. H. Cady, The PETN-DiPEHN-Tri-PEON System, Los Alamos, NM.: University of California; **1972**. LA-4486-MS. Available from NTIS, Springfield, VA.
8. T. Allen, Particle Size Measurement, vol. 2, Chapman & Hall, London, UK, 5<sup>th</sup> Edition, **1997**.
9. P. C. Carman, The determination of the specific surface of powders, *J. Soc. Chem. Ind. Trans.* **1938**, 57, 225.
10. J. Kozeny, Ueber kapillare Leitung des Wassers im Boden, *Wein. Akad. Wiss.* **1927**, 136 (2a), 271.
11. P. C. Carman, Flow of gases through porous media, Butterworths Scientific Publications, London, UK, **1956**.

12. E. L. Gooden, C. M. Smith, Measuring average diameter of powders — an air permeation apparatus, *Ind. Eng. Chem. Anal. Ed.* **1940**, *12*, 479.
13. E. Edmonds, A. Hazelwood, T. Lilly, and J. Mansell, Development of in-situ surface area analysis for detonators, *Powder Technology* **2007**, *174*, 42.
14. M. E. Moore *et al.*, PETN Aging and Reliability Study, PXRPT-10-04, **2010**.
15. A. Maiti and R. H. Gee, PETN Coarsening – Predictions from Accelerated Aging Data, *Propell. Explos. Pyrot.* **2011**, *36*, 125.
16. R. Pitchimani *et al.*, Thermodynamic analysis of pure and impurity ooped Pentaerythritol Tetranitrate crystals grown at room temperature, *J. Therm. Anal. Cal.* **2007**, *89*, 475.
17. G. W. Brown, M. M. Sandstrom, A. M. Giambra, J. . Archuleta, and D. C. Monroe, Thermal Analysis of Pentaerythritol Tetranitrate and Development of a Powder Aging Model, *NATAS Proceedings*, **2009**.
18. S. Bhattacharya, A. Maiti, R. H. Gee, J. Nunley, and B. L. Weeks, Effect of homolog doping on surface morphology and mass-loss rate from PETN crystals: studies using atomic force microscope and thermo-gravimetric analysis, *Propell. Explos. Pyrot.* **2013**, *35*, 1.

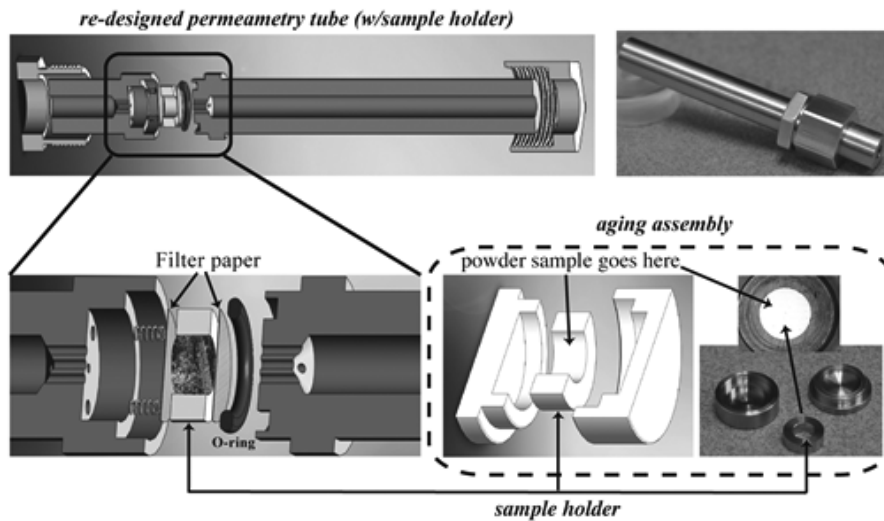


Fig. 1. Schematics of the re-designed permeametry tube, Invar sample holder and aging assembly; Invar, is an Fe-Ni alloy with very low coefficient of thermal expansion. The new sample holder can be conveniently transferred between an aging assembly (schematics shown within the dashed rectangle) and the re-designed permeametry tube with minimal mechanical disturbance of the powder sample, thus effectively enabling the *in-situ* monitoring of FSSA evolution of each sample as a function of age (time and temperature).

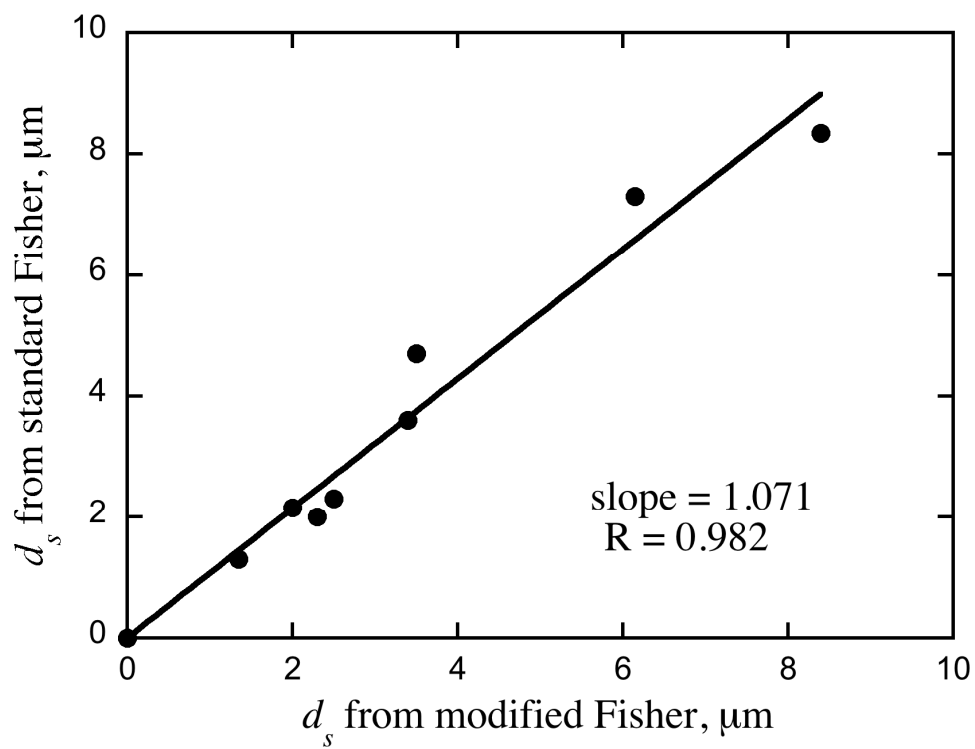


Fig. 2. Correlation between standard Fisher (using 1.78 g of powder) and modified-Fisher (using 111 mg of powder) measurements using eight different PETN powder samples. The slope (displayed in the figure) was used to recalibrate  $d_s$  from small-powder measurements using the modified-Fisher apparatus.

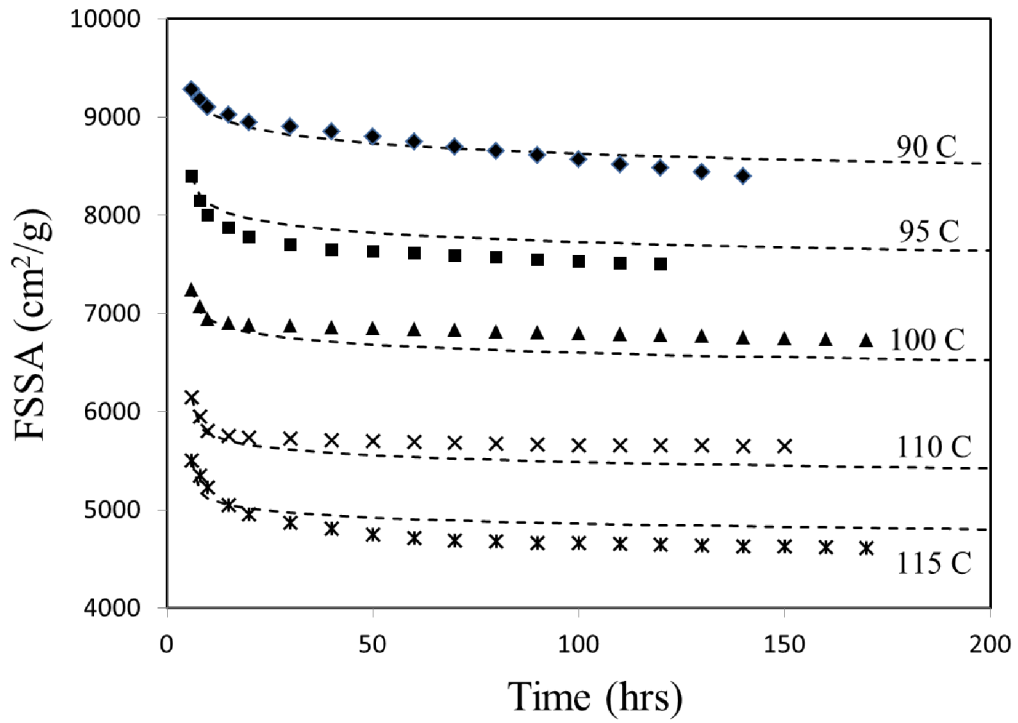


Fig. 3. Fitting of historical aging data of PETN from Ref. [15] with eqs.(7) and (8). Parameters used:  $\tau = 8.2 \times 10^{-22}$  hrs, and  $\alpha = 0.016$ . The coarsening time origin was taken at 6 hrs.

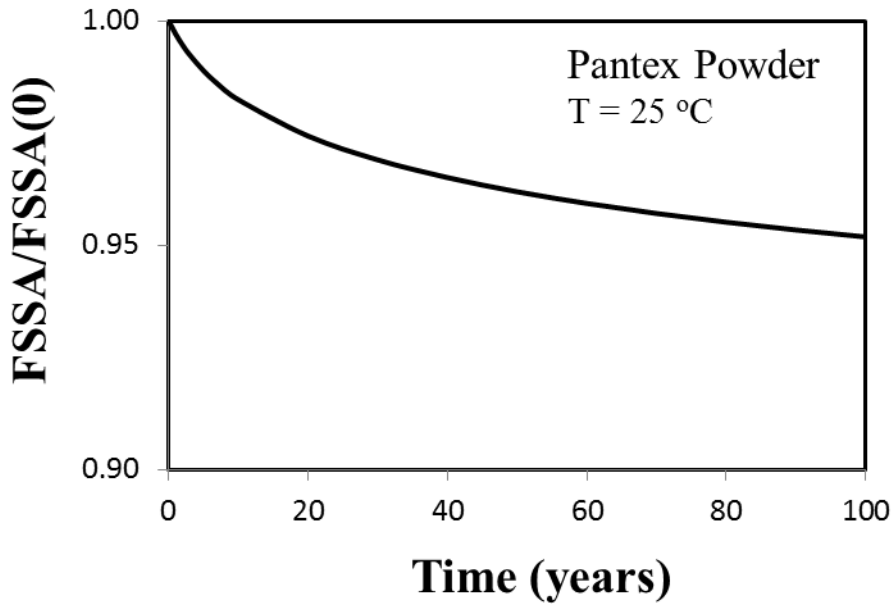


Fig. 4. Long-term prediction of specific surface area of the historical powder (as a fraction of the original starting FSSA at deployment) using our new aging model, eqs. (7) and (8).

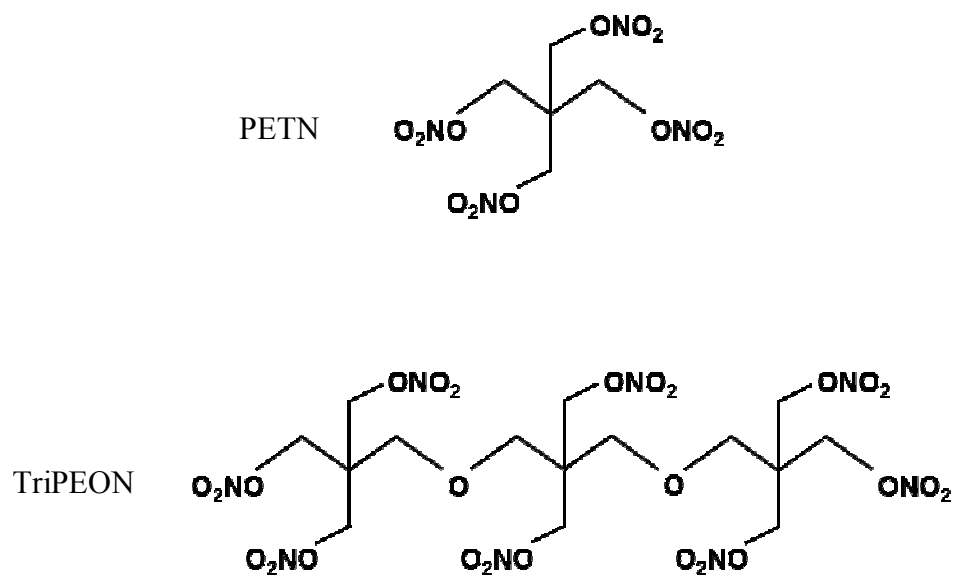


Fig. 5. Molecular stick diagrams of a PETN (pentaerythritol tetranitrate) and a TriPEON (tripentaerythritol octanitrate) molecule.

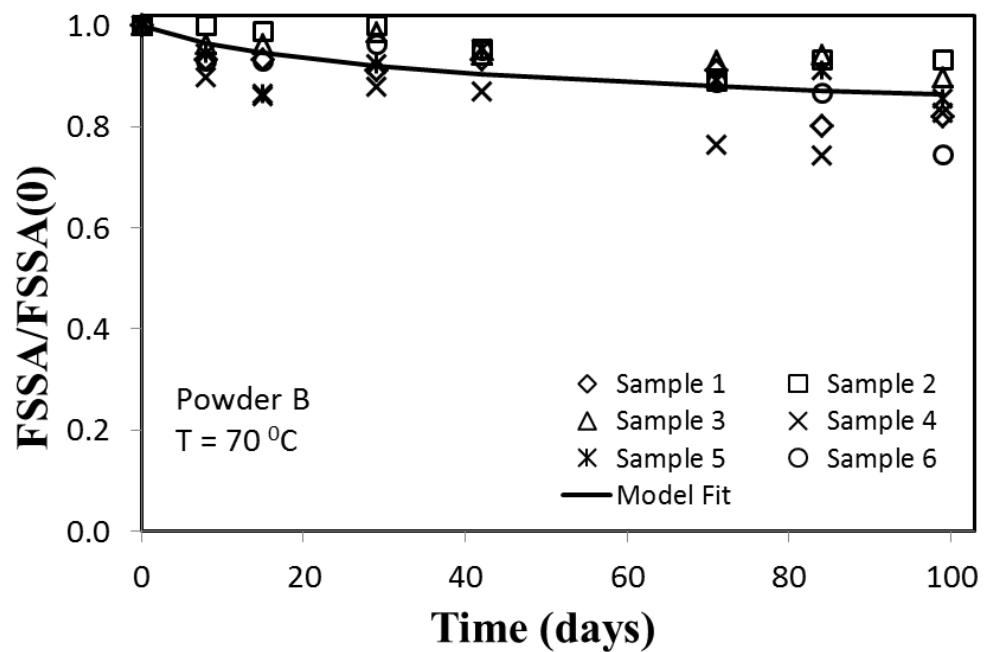
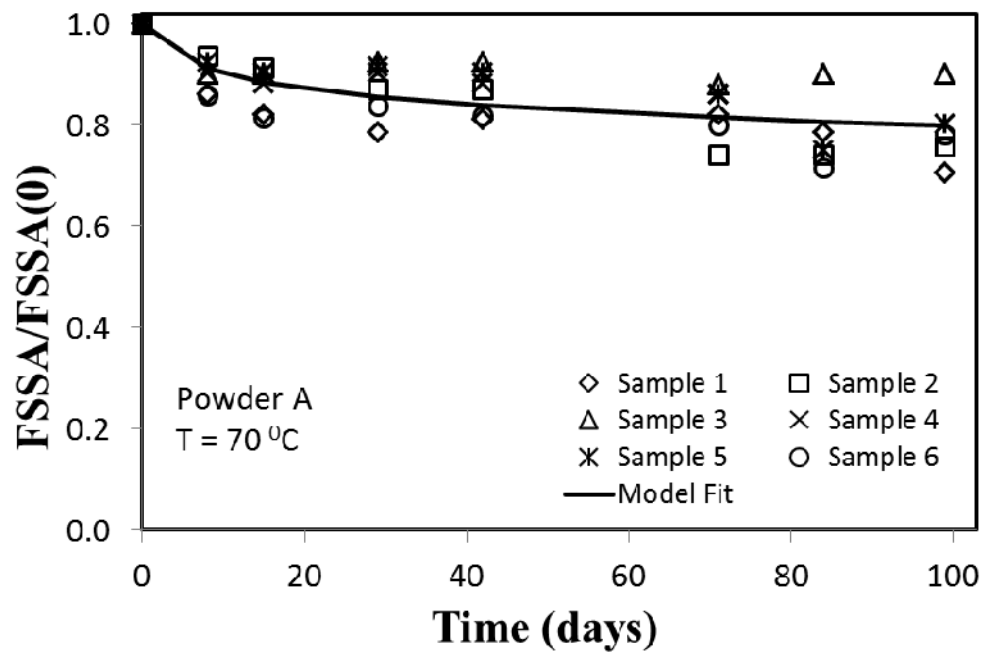


Fig. 6. Fractional change in specific surface area (FSSA) in pure-PETN powders A and B under accelerated aging at 70 °C over a period of about 100 days. The different symbols correspond to different samples, and the best model fit to the sample average indicated by solid line.

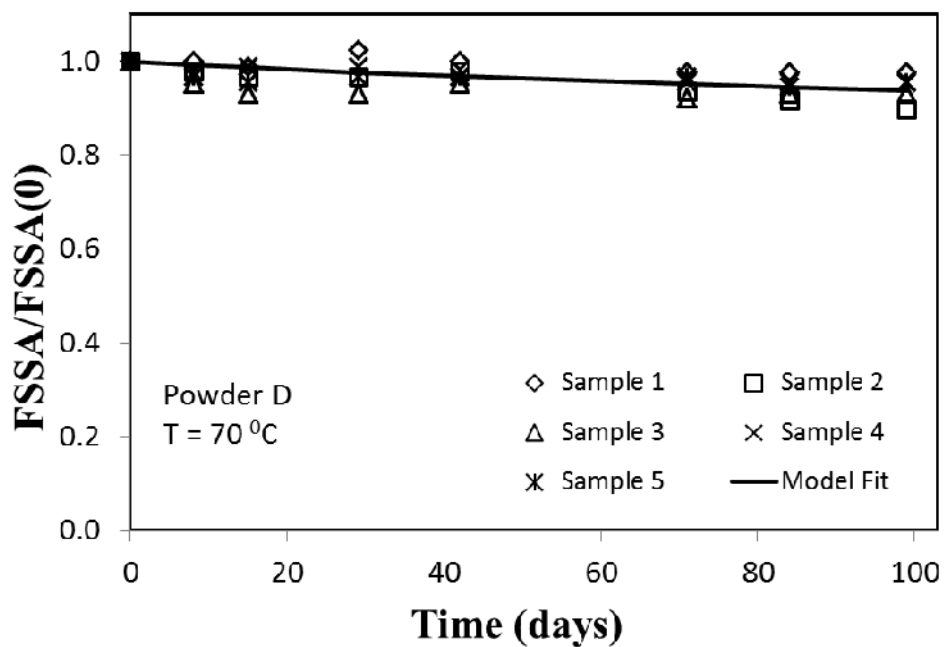
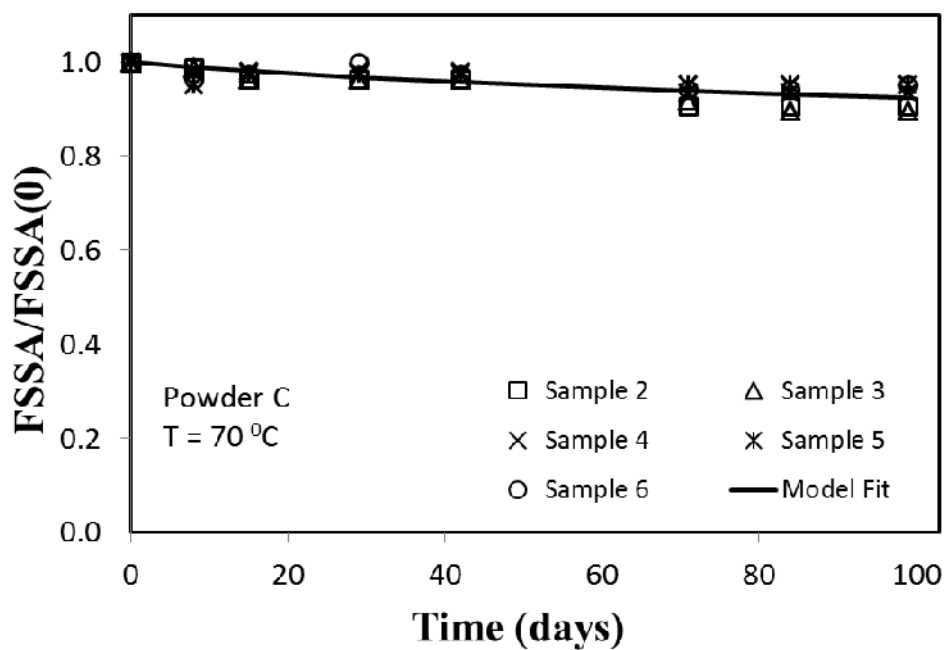


Fig. 7. Fractional change in specific surface area (FSSA) in powders C and D (PETN powders containing ~ 1 wt% TriPEON) under accelerated aging at 70 °C over a period of about 100 days. The different symbols correspond to different samples, and the best model fit to the sample average indicated by solid line.

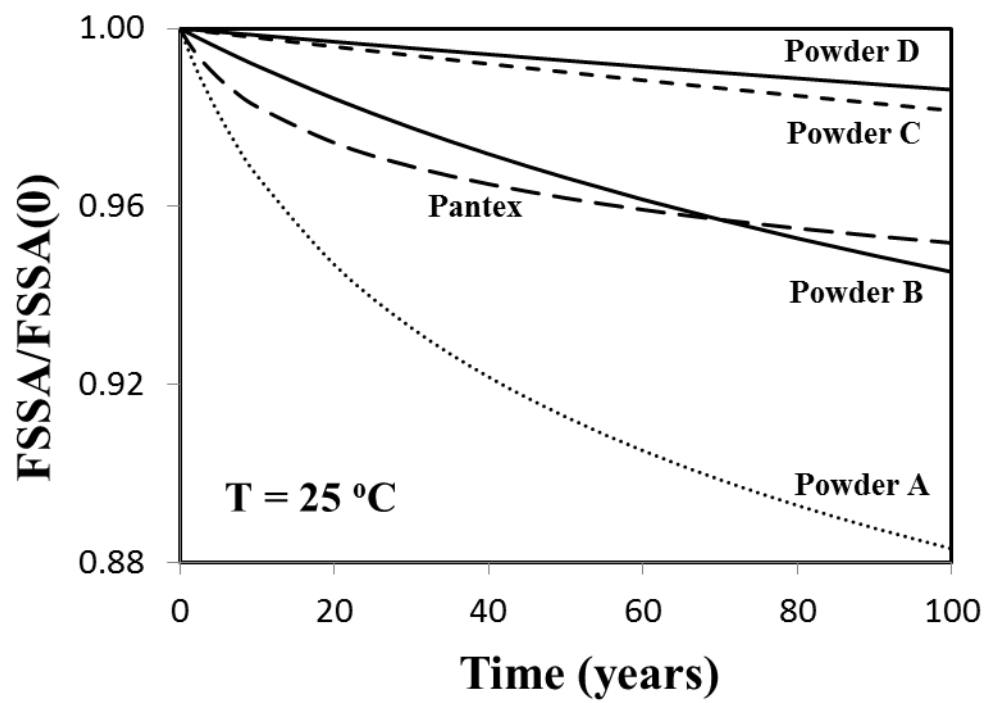


Fig. 8. Long-term aging predictions for five different powders from our aging model (eqs. (7) and (8)).